

Application of response surface methodology for the optimization of copper (II) adsorption in aqueous solution using rambutan peel powder biosorbent

N. L. Wei, S. R. B. Hassan*

*Faculty of Bioengineering and Technology, Universiti Malaysia Kelantan, Malaysia
Advance Industrial Biotechnology Cluster, Universiti Malaysia Kelantan, Malaysia*

Received: October 14, 2020; Revised: August 02, 2022

In this study acid-treated rambutan peel was used as a low-cost agricultural waste-derived biosorbent to remove copper (II) from aqueous solution. Central composite design (CCD) of response surface methodology (RSM) was applied to study the optimization of adsorption capacity and removal efficiency through analyzing the parameters (initial copper (II) concentration, pH and biosorbent dosage) by using Design-Expert software. The optimum conditions of adsorption capacity of copper (II) were: biosorbent dosage = 0.05 g, initial copper (II) concentration = 60 mg/L, pH = 5 whereas for removal efficiency they were: biosorbent dosage = 0.1 g, initial copper (II) concentration = 35 mg/L, pH = 5. The highest adsorption capacity and removal efficiency obtained were 25.33 mg/g and 95.24 %, respectively. Pseudo-first and -second order models and intra-particle diffusion model were applied to study adsorption kinetics. The kinetic data fitted well the pseudo-second order model with R^2 of 99.28 %. Characterization of raw and acid-treated rambutan peel biosorbent before and after adsorption was performed with FTIR, SEM and EDS.

Keywords: Adsorption, characterization, biosorbent, copper (II), kinetic studies.

INTRODUCTION

The significant water pollution issue has been identified to threaten humans and aquatic animals due to discharging inorganic chemicals without being properly purified. This issue could trigger toxicity to living organisms that accidentally consumed over permitted level. The industrial activities in agricultural field and petroleum effluents discharged massive amounts of effluents containing heavy metals into the drainage water stream which can lead to severe environmental effects and potential human exposure. High contents of heavy metal effluents to the environment can cause contamination to the groundwater and surface water with an increase in biochemical oxygen demand (BOD) and chemical oxygen demand (COD) levels that could disturb living of aquatic animals and diminish the crop yields. Barreto *et al.* [1] stated that the discharging of heavy metal effluents in sedimentation of freshwater credited to the deposition of metal elements that altered chemical configuration of anthropogenic impacts and supplementation of aquatic plants. Lead poisoning may lead to damage of nervous system which can trigger irritability, headache, loss of memory and poor attention span to humans [2]. Copper is the third most necessary trace element following iron and zinc which functions as a catalyst to speed up heme synthesis and adsorption of iron by human body. Copper is categorized as a metal with high electrical and thermal conductivity. It is also less corrosive and has

the properties of alloying and malleability [3]. Copper can be used as a therapeutic mediator which has the advantage to treat Alzheimer's disease and Parkinson's disease when used in the correct approach of treatment [4]. Therefore, heavy metals like copper are essential in development and redox chemistry in the living organisms in acceptable quantities which are non-toxic. Excessive intake of copper by the human body can trigger Wilson's disease [5]. It is an uncommon autosomal recessive disorder which occasions in toxicity to liver and brain damage. Drinking water that is obtained from contaminated water source is the major reason for copper toxicity in the human body. Moreover, the serum copper absorption was scaled up to nearly 1.5 mg/L for a health-giving person [3].

Environmental pollution regarding the discharging of toxic heavy metals from industrial effluents to the environment has been greatly concerned by the public. Hence, effective actions should be taken to guarantee the prospect of mankind protection. Ahmad [6] stated that all metals have the properties of bio-availability and solubility at low pH, which are more critical in acidic environment. Heavy metals like chromium, lead and mercury have carried toxicity and harmful effects to the living organisms when transmitted into the environment.

Copper (II) composites are widely applied in various commercial activities, for instance the leather tanning and textile dyeing processes in the

* To whom all correspondence should be sent:
E-mail: roshayu.h@umk.edu.my

industry. Copper (II) can act as a fundamental nutrient for various living organisms in regulated amounts. High level of copper (II) contents can lead to poisonous and mutagenic effects. Moreover, excessive consumption of lead can cause kidney damage which affects the effectiveness of kidney and leads to renal failure in human body. The highest acceptable toxicity of inorganic lead is identified to scale from 0.04 to 0.198 mg/L depending on the different conditions [7]. Even though there are many techniques for the removal of heavy metals, they are mostly still in laboratory scale and only few are successfully applied to the industrial level. Therefore, effective methods are required to preserve the aquatic environment from pollution of heavy metals. The adsorption using wastes generated from agricultural and food industry can efficiently remove heavy metal ions as the heavy metals will attach to the surface of the biological materials. Biological resources with high metal binding ability are beneficial in adsorption process. The significance of bio-waste products in removing heavy metals ions from the wastewater is essential.

A biosorbent is a natural resource that can be used to eliminate toxic heavy metals from wastewater sources. A cost-effective biosorbent has the advantages of needing little processing procedures and is originally obtained from wastes that are beneficial in reducing environment pollution problems. Therefore, it is essential to study on new sources of bio-sorbents to remove heavy metals in industrial effluents. The rambutan peels have been used to effectively remove malachite green dyes in the form of activated carbon. There are still not many studies on the rambutan peels as a biosorbent to remove heavy metals. The previous research study only investigated the removal of malachite green dyes using activated carbon from rambutan peels [8, 9].

MATERIALS AND METHOD

Biosorbent

The collected raw rambutan (*Nephelium lappaceum*) peel samples were rinsed with water, air-dried, cut into smaller size and acid-treated with 0.1N sulfuric acid. The acid-treated sample was dried, grinded and sieved. The raw and acid-treated rambutan peel powder samples were kept in separated zip bags.

Experimental design

Central composite design (CCD) of the response surface methodology (RSM) was used for the experimental design. Table 1 shows the experimental runs generated from CCD to study the

adsorption of copper (II) by the biosorbent. The 'low' and 'high' in the table indicates the lower limit and higher limit of tested parameters, respectively. The pH, initial copper (II) concentration and biosorbent dosage were designed as the variables A, B, and C, respectively. The ranges used were taken after preliminary testing carried out for each variable. The 20 sets of experimental runs which were designed and generated from CCD according to Table 2 were used to carry out the adsorption studies to determine the removal of copper (II) by the biosorbent. The removal percentage and adsorption capacity of copper (II) were calculated using eq. (1) and eq. (2), respectively, and Design-Expert software to obtain the optimum conditions for removal of copper (II).

Table 1. Experimental runs for adsorption studies.

Variables	Units	Low (-1)	High (+1)
A: X ₁		2	8
B: X ₂	mg/L	10	60
C: X ₃	g	0.05	0.15

Table 2. Experimental design for adsorption studies using CCD.

No.	A	B (mg/L)	C (g)
1	8	10	0.05
2	8	10	0.15
3	2	10	0.05
4	5	10	0.1
5	2	10	0.15
6	5	35	0.15
7	5	35	0.1
8	5	35	0.05
9	2	35	0.1
10	5	35	0.1
11	8	35	0.1
12	5	35	0.1
13	5	35	0.1
14	5	35	0.1
15	5	35	0.1
16	5	60	0.1
17	2	60	0.05
18	8	60	0.15
19	8	60	0.05
20	2	60	0.15

Optimization of adsorption

The acid-treated rambutan peel powder was used as biosorbent to optimize the adsorption of copper (II). Constant were kept the agitation speed (150 rpm), temperature (30 °C), volume of copper (II) solution (100 ml) and contact time (45 minutes). The effects of pH, initial copper (II) concentration and biosorbent dosage on removal percentage and adsorption capacity of copper (II) were studied. 20 runs of adsorption studies were carried out according to Table 2 which was generated using the Design

Expert software. The absorbance readings were obtained by UV-Vis spectrophotometry at 580 nm. The reacted mixture from each set of adsorption studies was filtered using a filter paper to obtain a clear solution. Three replicates were obtained from each of the 20 sets of adsorption studies in order to increase the accuracy of the results. The concentration of copper (II) was controlled by means of a standard calibration curve. The adsorption capacity at equilibrium, q_e , was calculated using eq. (1):

$$q_e \left(\frac{mg}{g} \right) = \left[\frac{C_i - C_e}{m} \right] V \quad (1)$$

where C_i is the initial concentration of copper (II) in aqueous solution, C_e is the final concentration of copper (II) in aqueous solution (mg/L), m is the mass of biosorbent (g), and V is the volume of solution (L). The removal percentage efficiency was calculated using eq. (2):

$$R(\%) = \left[\frac{C_i - C_e}{C_i} \right] \times 100 \quad (2)$$

where C_i is the initial concentration of copper (II) in aqueous solution, C_e is the final concentration of copper (II) in aqueous solution (mg/L).

Kinetic studies

The mathematical models used in this study for describing the kinetics of adsorption were determined by using pseudo-first and -second order kinetics, as well as intra-particle diffusion model. The kinetic studies are of significance to study the behavior of the adsorption to optimizing the adsorption properties. The pseudo- first and -second order models and intra-particle diffusion model were applied using eq. (3), eq. (4) and eq. (5), respectively. Eq. (3) shows the linearized pseudo-first-order model:

$$\log(q_e - q_t) = \frac{k_1}{2.303} t \quad (3)$$

where, q_e is the amount of biosorbent at equilibrium (mg/g), q_t is the amount of biosorbent at equilibrium (min) and k_1 is the rate constant (1/min). The pseudo-second order model was applied using eq. (4). Eq. (4) shows the linearized form of pseudo-second order model:

$$\frac{t}{q_t} = \frac{1}{k_2 q_e^2} + \frac{1}{q_e} t \quad (4)$$

where, q_e is the amount of biosorbent at equilibrium (mg/g), q_t is the amount of biosorbent at equilibrium (min) and k_2 is the rate constant (mg/g). The intra-particle diffusion model was applied using eq. (5). Eq. (5) shows the linearized form of the intra-particle diffusion model:

$$Q_t = K_{id} t^{0.5} + C \quad (5)$$

where, Q_t is the amount absorbed at time t and $t^{0.5}$ is the square root of the time, C is the intercept and K_{id} ($mg\ g^{-1}\ min^{-0.5}$) is the rate constant of intra-particle diffusion.

Analysis and characterization

The characterization of rambutan peel powder was carried out using Fourier transform infrared spectroscopy (FTIR), scanning electron microscopy (SEM) and energy dispersive X-ray spectroscopy (EDS) which were used to study the major functional groups, composition and topography of biosorbent and semi-quantitative elemental materials on specific sites within the observed area of rambutan peel biosorbent.

RESULTS AND DISCUSSION

Characterization of rambutan peel biosorbent

Surface morphology and elemental composition analysis. From Fig 1(A) it is seen that acid-treated rambutan peel biosorbent has obtained additional pores on the surface compared to raw rambutan peel biosorbent, though it did not demonstrate a consistent structure of biosorbent surface. The surface of acid-treated rambutan peel biosorbent after adsorption displayed more porous structure compared to before adsorption. After acid treatment, the rambutan peel biosorbent displayed to be more heterogeneous and multiplex compared to raw rambutan peel biosorbent with a relatively smooth surface.

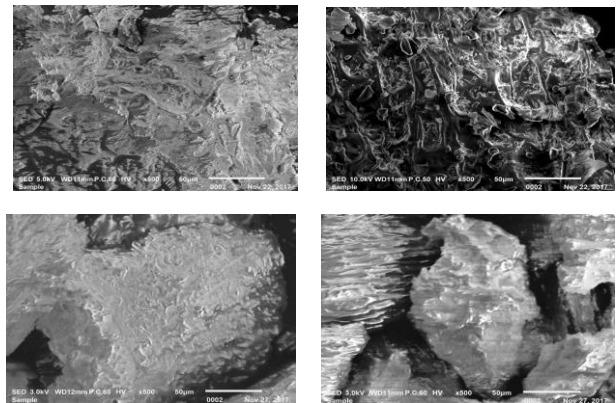


Figure 1. SEM image of acid-treated rambutan peel powder before adsorption (a), acid-treated rambutan peel powder after adsorption (b), raw rambutan peel powder before adsorption (c), and raw rambutan peel powder after adsorption (d).

From the results of SEM analysis it followed that acid-modified biosorbent after adsorption was composed of hollow and favorable porous carbon fibers encircled with masses of carbon composites

[10]. However, the raw rambutan peel biosorbent did not display an obvious metamorphosis before and after adsorption process. Moreover, it can also be monitored that adsorption is a surface spectacle. This is due to the fact that smaller biosorbent particle sizes provide a moderately greater and additionally available surface area with additional pores acquired [11]. In consequence, a better adsorption mechanism can take place at equilibrium. EDS analysis was carried out to determine the chemical composition available on the surface of rambutan peel biosorbent. Both acid-treated and raw rambutan peel biosorbent displayed a low distinct peak of copper (II) loaded before adsorption (see Fig. 2 (A) and (B)), whereas the spectrum has clearly displayed incidence of copper (II) present for both raw and acid-treated rambutan peel biosorbent surfaces after adsorption (Fig. 2 (C) and (D)). The peak of copper appeared to be greater after the adsorption process as compared to raw rambutan peel biosorbent before adsorption which indicates that an adsorption process of copper (II) took place at the surface of rambutan peel biosorbent. Moreover, the increased peak of copper (II) in acid-treated rambutan peel biosorbent after adsorption in Fig. 2 (D) describes the chemical composition appeared on the surface of acid-treated rambutan peel biosorbent. As estimated, EDX spectra proved that the carbon content has highest percentage in the existence of diatoms. Nonetheless, oxygen, calcium, phosphorus and silicon are also present in each spectrum. This may be due to the precipitated compounds present, dissolved substances and salts present during the adsorption process of copper (II) [12]

Fourier transform infrared spectroscopy (FTIR) analysis. FTIR spectrum clarifies the functional groups available in the adsorption of copper (II) by rambutan peel biosorbent. The model of adsorption of copper (II) is due to the presence of active functional groups. Presence of distinct peaks at 1317.00 cm^{-1} and 1613.14 cm^{-1} in Fig. 3 (A) specified the presence of C-O stretch in carboxylic acids and N-H bends in amine groups for the adsorption process. The existence of C-C triple bond of alkynes at the peak 2296.03 cm^{-1} clearly specifies the contribution of alkynes in adsorption of copper (II). Thus, it is obvious that carboxylic acids, amines and alkynes are involved in the adsorption of copper (II).

The multiplex spectra of acid-treated rambutan peel biosorbent in Fig. 3 (B) after adsorption display some strong adsorption bands. The broad peak at 1017.74 cm^{-1} represents the existence of C-F stretch of C-bonded in alkyl halides. The alteration of this peak after adsorption points at the contribution of C-

F groups from alkyl halides. The disappearance of the peak at 1316.42 cm^{-1} after adsorption (see Fig. 3 (B)) is a proof of the contribution of C-H stretch in alkene group.

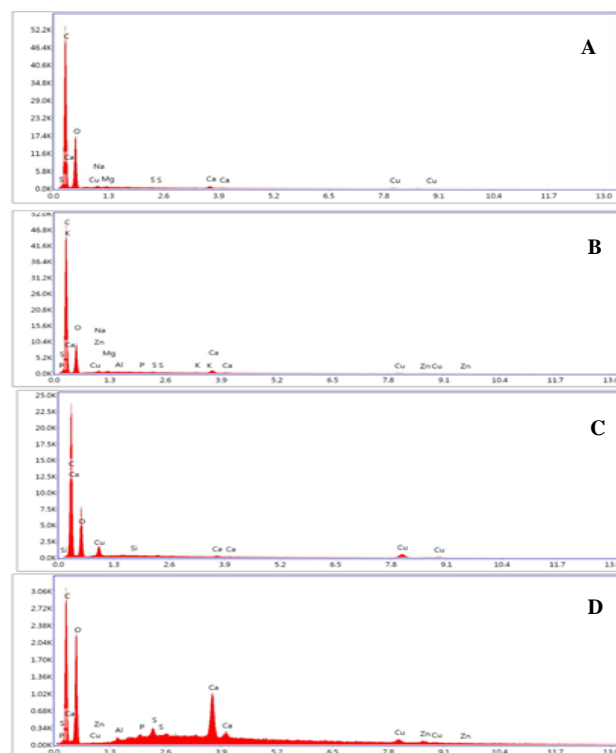


Figure 2. EDS image of acid-treated rambutan peel powder before adsorption (a), raw rambutan peel powder before adsorption (b), raw rambutan peel powder after adsorption (c) and acid-treated rambutan peel powder after adsorption (d).

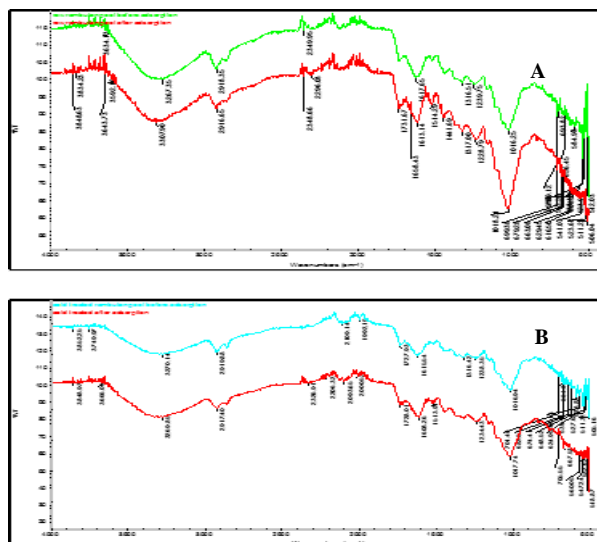


Figure 3. FTIR spectra for raw rambutan peel powder before and after adsorption (a) and acid-treated rambutan peel powder before and after adsorption (b)

The peak at 3749.97 cm^{-1} corresponds to acetylenic C-H stretch of alkyne group and the decline of the peak at 3666.05 cm^{-1} after adsorption

means that the alkyne group has affected intensely the adsorption of copper (II). The peak at 2206.03 cm^{-1} specifies the existence of C-C triple bonding stretch in alkyne groups which also affected the adsorption of copper (II). In Fig. 3 (B), a definite peak at 1016.94 cm^{-1} before adsorption relates to S=O stretch in sulfoxide group and its decline after adsorption of copper (II) specifies the contribution of particular groups in adsorption process [13]. The peak at 683.63 cm^{-1} is a suggestion for contribution of C-Cl stretch in alkyl halide groups for adsorption of copper (II). Consequently, the major functional groups of acid-treated rambutan peel biosorbent that affected the adsorption of copper (II) are found to be alkyl halides, alkenes, carboxylic acids, alkynes and sulfoxide groups.

Response surface methodology

Removal efficiency. Response surface methodology creates an empirical model articulated through a second-order polynomial equation in terms of the coded factors. This relationship reflects the correlation between variables concerning the response. The coefficient with one factor indicates the consequence of specific variable, therefore the coefficient with two factors together with the second-order term will affect the correlation between these two factors, as well as the quadratic effect, correspondingly.

Through pertaining multiple regression evaluation on the design matrix and response, the equation of the removal percentages of copper (II) in terms of coded factors is as shown below:

$$\text{Removal percentages} = 90.52 - 3.06A - 2.19B + 0.75C - 2.5AB - 0.97AC + 0.56BC - 1.97A^2 + 1.32B^2 - 9.16C^2 \quad (6)$$

where, A is the initial copper (II) concentration, B is the biosorbent dosage and C is the pH.

A plot of observed percentage probability of the residuals to the predicted probability is represented in Fig. 4. The observed percentage probability of the residuals represents approximately no significant interruption of the expectations underlying the studies. It authorizes the normality expectations composed in advance, as well as the independence of the residuals through presenting a fitting normal distribution. There is an adequate relationship between the observed probability and the predicted probability of the copper (II) removal percentage as shown in Fig. 4. The points assembled around the sloping line on the graph represents a good fit of the quadratic model, subsequently the deviation among the observed and predicted values was lower [14, 15].

The outcomes of the second-order response

surface model in the formula of investigation of variance (ANOVA) are presented in Table 3. The statistical significance of the model equation was evaluated by the F-test ANOVA. The significance of each coefficient was regulated by F-values and P-values. It is seen from Table 3 that the coefficients for the main and square effects are highly significant ($P < 0.0001$) in comparison with interaction effects. Table 3 displays ANOVA for the response surface quadratic model.

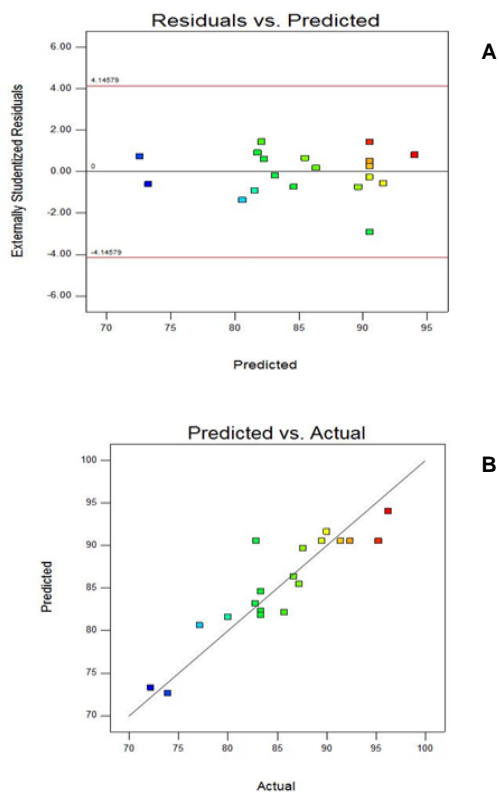


Figure 4. Plot of residuals to predicted probability (A) and plot of actual probability to predicted probability (B)

Table 3. Regression analysis using central composite design

Factor	Coefficient estimation	df	Stand. error	F-value	P-value
Intercept	2.99	1	0.87	11.99	0.0003
A	6.49	1	0.80	65.33	<0.0001
B	-2.69	1	0.80	11.22	0.0074
C	0.01	1	0.80	0.00	0.9891
AB	-2.39	1	0.90	7.08	0.0238
AC	0.61	1	0.90	0.46	0.5115
BC	-0.28	1	0.90	0.10	0.7633
A ²	1.85	1	1.53	1.46	0.2550
B ²	0.29	1	1.53	0.04	0.8521
C ²	4.01	1	1.53	6.88	0.0255

The F-value (65.33) for factor A with a low probability value ($P < 0.0001$) demonstrates a high

significance for the regression model. The goodness of the fit of the model was also checked *via* the multiple correlation coefficient (R^2). In this study, the value of the multiple correlation coefficient was 0.8313, which means that this regression is statistically important and 16.87% of the complete variations is not described *via* the quadratic model. The value of predicted multiple correlation coefficient (pred. $R^2 = 0.3733$) is not equally adjacent to the compact in conjunction with the value of the adjusted multiple correlation coefficient (adj. $R^2 = 0.6794$). Simultaneously, a comparatively inferior value of the coefficient of variance ($CV = 4.32\%$) specifies an improved accuracy and dependability of the tests conducted.

Effect of pH and initial copper (II) concentration. An upsurge of removal efficiency of copper (II) through increasing the initial copper (II) concentration is a consequence of the enhancement in the impelling cause of concentration gradient, moderately increasing in the initial copper (II) concentration. As the initial copper (II) concentration is greater, the active sites of the rambutan peel biosorbent would be encircled with high amount of copper (II) ions, hence the adsorption process can be conducted more frequently and adequately to reach the optimization of the adsorption process. Consequently, the gradual increase of the pH value and initial copper (II) concentration up to the optimized conditions will effectively enhance the adsorption process. Moreover, some researchers have also studied the effect of pH with initial copper (II) concentration for adsorption of heavy metals using different kinds of biosorbent and the results agreed with this study. Cekim *et al.* [16] stated an increased adsorption efficiency (q_e) from synthetic water through tobacco leaf absorbent on increasing the initial copper (II) concentration with the reading of greatest q_e (10.66 mg/g) with initial copper (II) concentration of 50 mg/L. In a study of the adsorption of copper using *tamarindus indica* fruit nut testa as biosorbent, maximum adsorption level was achieved at pH 5 for copper and the effect of pH can be interpreted on the basis of the structure of biosorbent and speciation of copper [17].

Effect of biosorbent dosage and pH. The effect of pH and biosorbent dosage on the removal efficiency of the copper (II) is displayed in Fig. 6. It was found that the removal efficiency of copper (II) decreased with increasing biosorbent dosage from 0.05 to 0.15 g and its optimum value was recorded as 0.1 g. The actual factor of initial concentration recorded was 35 mg/L. In order to explain based on the experimental researching, increasing biosorbent dosage can be

recognized as a contribution to the increasing of the surface area for the adsorption of copper (II), as well as the accessibility of additional adsorption sites. Nonetheless, the removal efficiency will decrease with the increasing of biosorbent dosage. This is due to the reason that the initial factor describing the situation is that adsorption sites stay unsaturated throughout the adsorption process and the amount of active sites accessible for adsorption increased through the enhancing of biosorbent dosage.

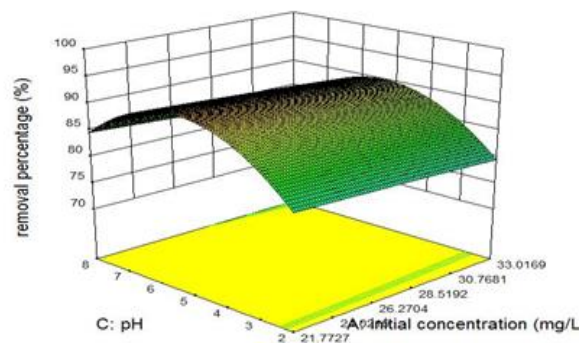


Figure 5. Response surface plot of the effect of pH and initial copper (II) concentration.

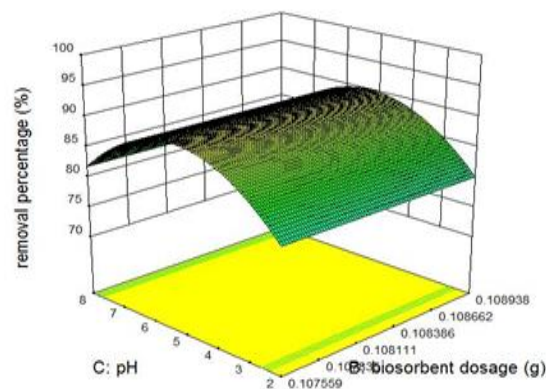


Figure 6. Response surface plot of the effect of biosorbent dosage and pH

Validation of regression model equation

For the development of a regression model equation, three variables were considered as independent process variables. Their discrete and interactive properties on the removal efficiency of copper (II) as a response were studied using central composite design. A quadratic polynomial model was applied in order to regulate the correlation between the process factors and its corresponding response. No transformation was needed and the quadratic model was selected to fit the data as

recommended by the Design Expert 10.0.7 software. The expedient alternative of central composite design is the face-positioned design which is a three-level design for response surface studies to be carried out. It will map out the shapes of quadratic surface and show results in optimization of the variables to the removal percentages. This design is located at axial points of the centers of cube faces as shown in Fig. 7 which has $k=3$ factors. The variation of central composite design was applied due to the requirement of three levels of factors.

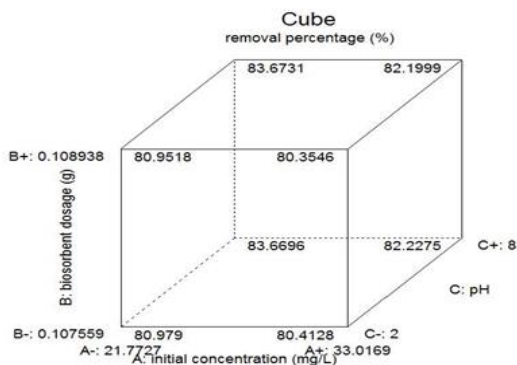


Figure 7. Face-centred central composite design for $k=3$.

Absorption capacity

Effect of pH and initial copper (II) concentration.

The effects of pH and initial copper (II) concentration on the adsorption capacity by acidic treated rambutan peel biosorbent can be observed in Fig. 8. The adsorption capacity of copper (II) increased with the increase in initial copper (II) concentration of 10 to 60 mg/L together with pH ranging from 2 to 8. The highest adsorption capacity of copper (II) was determined to be 24 mg/g. Hence, the excessive pH condition will reduce the adsorption capacity of copper (II). When the initial copper (II) concentration increases, there will be an increase in the adsorption capacity due to the driving force of the copper (II) concentration gradient. As the same situation, the more copper (II) ions present in the adsorption, the active sites of biosorbent would be encircled with high concentration of copper (II). In consequence, the adsorption capacity would be more efficient [18]. The adsorption capacity increased when the pH condition increased. The adsorption capacity achieved maximum at greater pH values and decreased as the pH condition was further excessive. The pH condition will equally affect surface binding sites and chemical properties on the biosorbents [19].

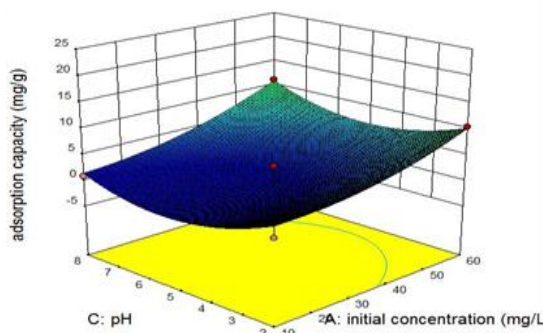


Figure 8. Response surface plot of effect of pH and initial copper (II) concentration.

Effect of initial copper (II) concentration and biosorbent dosage. The effects of initial copper (II) concentration and biosorbent dosage on the adsorption capacity by acidic treated rambutan peels biosorbent can be observed in Fig. 9. The adsorption capacity of copper (II) increased with the increased of initial copper (II) concentration of 10 to 60 mg/L together with biosorbent dosage ranged from 0.05 to 0.15 g. The highest adsorption capacity of copper (II) was determined to be 24 mg/g. With the lower biosorbent dosage and higher initial copper (II) concentration, there is a higher adsorption capacity recorded. This is due to the higher ratio of biosorbent surface binding sites to the copper (II) concentration presented during the adsorption mechanism. From Fig. 9, the biosorbent dosage increased with the decreasing of adsorption capacity of copper (II) per unit mass of biosorbent (q_e) [20]. The increasing of biosorbent surface active binding sites and accessibility of more adsorption active sites are interdependent to the increasing in biosorbent dosage in the study. Yet the adsorption capacity (q_e) will decrease with increasing of biosorbent dosage, as seen from Fig. 9. As a result of the situation, the adsorption active binding sites of biosorbent will be maintained unsaturated during the adsorption mechanisms although the quantity of active sites obtainable for adsorption increased with increased biosorbent dosage.

Perturbation plot

Perturbation plot illustrations of the function of particular actual factors countered as the level of particular factor altered while the other factors were stable at optimum conditions. The steeper slope in the perturbation plot represents the sensitivity of response factors.

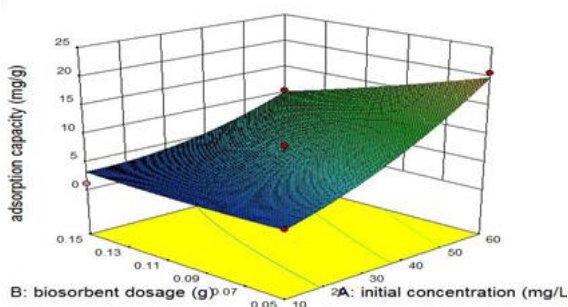


Figure 9. Response surface plot of the effect of initial copper (II) concentration and biosorbent dosage.

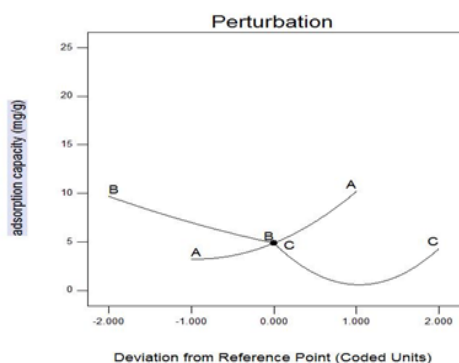


Figure 10. Perturbation plot of the adsorption capacity of copper (II) with actual factors, A: initial copper (II) concentration, B: biosorbent dosage and C: pH.

Therefore, perturbation plot of adsorption capacity of copper (II) was applied to evaluate the consequences of respective factors on the adsorption capacity of copper (II). From Fig. 10, the biosorbent dosage decreases while the initial copper (II) concentration and pH values increases as the adsorption capacity of copper (II) was increased. Hence, it indicated that factors such as initial copper (II) concentration and pH would significantly impact on the adsorption capacity of copper (II). Through analyzing the slope of each factor from Fig 10, initial copper (II) concentration (A) and biosorbent dosage (B) are the major influential factors for the adsorption capacity of copper (II) as compared to pH (C). The adsorption capacities obtained for factor A and B were comparatively higher than for factor C. The relations of these factors have important effect on the responses [21].

Kinetics studies on adsorption

Adsorption process through biosorbent can be regulated with various types of mechanisms, for instance chemical reactions, diffusion control, and particle diffusion. Several adsorption models for

adsorption were utilized to interpret the experimental data obtained. Pseudo-first and -second order reaction kinetic models and intra-particle diffusion model were considered and fitted with the experimental data obtained. Figs. 11 and 12 display the plots of pseudo-first and -second order kinetic models for the adsorption of copper (II) through rambutan peel biosorbent, respectively. Experimental and hypothetically analyzed adsorption capacities at equilibrium (q_e) values and coefficients associated to kinetic plots are listed in Table 4. It can be observed from Table 4 that the linear correlation coefficients for pseudo-first order model are not well fitted with R^2 of 92.43 % compared to pseudo-second order model with R^2 of 99.28. These findings recommend that adsorption of copper (II) by rambutan peel biosorbent is not fitting to pseudo first-order reaction with lower R^2 value. It is apparent from the findings for correlation coefficients for pseudo-second order model that the adsorption of copper (II) is comparatively high with R^2 value of 0.9928 and the experimental and hypothetical adsorption capacities values are fitted well. Hence, the adsorption of copper (II) by rambutan peel biosorbent obeys the pseudo-second order model with R^2 of 99.28 %.

Furthermore, the intra-particle diffusion model predicts that overall adsorption rate is regulated by the rate of copper (II) diffusion within biosorbent pores [22]. It also determines the rate-limiting phase in adsorption of copper (II) in this study. Fig. 13 displays that adsorption of copper (II) is described by a linear graph which indicates that there is better agreement in the adsorption process. Adsorption mechanism is a multi-step progression as it develops two zones. In the first zone there is immediate adsorption whereas the second zone is steady adsorption phase [23]. The immediate adsorption is also known as external adsorption process which occurs at the external surface of biosorbent. The R^2 value of intra-particle diffusion model on adsorption of copper (II) was determined to be 95.95 % which means that 4.05 % of variation was not described by this model.

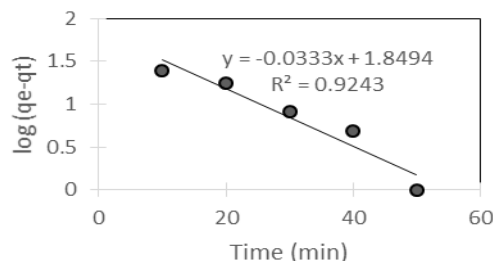


Figure 11. Pseudo-first order model plot for adsorption of copper (II) by rambutan peel biosorbent.

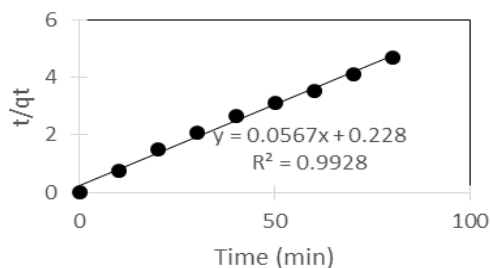


Figure 12. Pseudo-second order model plot for adsorption of copper (II) by rambutan peel biosorbent

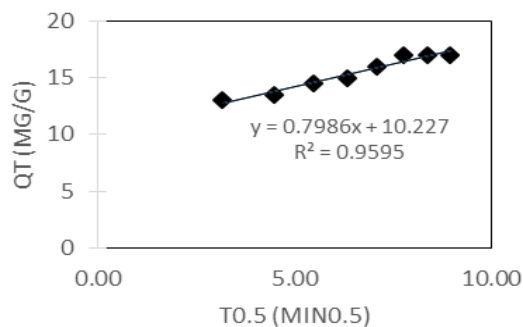


Figure 13. Intra-particle diffusion model plot for adsorption of copper (II) by rambutan peel biosorbent.

Table 4. Adsorption kinetic model rate constants of copper (II) removal by rambutan peel biosorbent

Kinetics	Pseudo-first order model	Pseudo-second order model	Intra-particle diffusion model
Q _e (mg/g)	70.697	17.637	
K (1/min)	0.0767	0.0141	
R ²	0.9243	0.9928	0.9595
Y-intercept			10.227
K _{id}			0.7986

CONCLUSION

The current study has determined that acid-treated rambutan peel biosorbent has adsorption capability towards copper (II) in aqueous solution. The parameters in terms of initial copper (II) concentration, biosorbent dosage and pH affected the removal efficiency of copper (II) from aqueous solution. From the 3D plots generated by RSM using Design-Expert software, it can be concluded that removal efficiency in terms of percentage increased as initial copper (II) concentration and pH increased, whereas it decreased as biosorbent dosage increased. The optimum condition for acid-treated rambutan peel biosorbent in adsorption of copper (II) was determined to be 35 mg/L initial copper (II)

concentration, pH 5 and 0.1 g of biosorbent dosage that gives removal efficiency as high as 95.24 %. Optimal adsorption capacity of copper (II) of 25.33 mg/g was obtained with RSM using Design-Expert software. Adsorption capacity of copper (II) increased along with increased initial copper (II) concentration and it decreased as biosorbent dosage and pH increased.

Pseudo-first and -second order model and intra-particle diffusion model were applied to study the adsorption kinetics of copper (II). The kinetic study models on adsorption of copper (II) were verified through the values obtained for determination (R²). Kinetic study on adsorption of copper (II) was performed to follow pseudo-second order model with R² of 99.28 % as compared to pseudo-first order model with R² of 92.43 % and intra-particle diffusion model with R² of 95.95 %. The value of R² with 99.28 % represents that 0.72 % of variation was not described by the pseudo-second order model. The consequence of the study indicated that acid-treated rambutan peel biosorbent is a potential biosorbent for the adsorption of copper (II) in aqueous solution. The kinetic study of adsorption of copper (II) described that both adsorption studies and intra-particle diffusion methods were applicable in adsorption of copper (II) using acid-treated rambutan peel biosorbent.

Acknowledgement: The authors wish to acknowledge financial support from Fundamental Research Grant Scheme (FRGs) of Malaysia (Ref no. FRGS/1/2021/TK0/UMK/02/6).

REFERENCES

1. W. J. Barreto, S. R. G. Barreto, I. S. Scarminio, F. Inoue, *Analytical Letters*, **43**(5), 814 (2010), <https://doi.org/10.1080/00032710903486278>
2. F. Fernández-luqueño, F. López-Valdez, P. Gamero-Melo, S. Luna-Suarez, E. N. Aguilera-González et al., *African Journal of Environmental Science and Technology*, **7**, 567 (2013), <https://doi.org/10.5897/AJEST12.197>
3. J. R. Turnlund, *Am. J. Clin. Nutr.*, **67**, 960 (1998).
4. F. Harris, L. Pierpoint, *Medicinal Research Reviews*, **29**(6), 1292 (2012), <https://doi.org/10.1002/med>
5. P. G. Georgopoulos, A. Roy, J. Yonone-Lioy, R. Opiekun, P. J. Lioy, *Journal of Toxicology and Environmental Health: Critical Reviews*, **4**(4), 341 (2001). <https://doi.org/10.1080/15287390500196230>
6. M. A. Ahmad, R. Alrozi, *Chemical Engineering Journal*, **168**(1), 280 (2011), <https://doi.org/10.1016/j.cej.2011.01.005>
7. M. R. Tayab, Environmental Impact of Heavy Metal Pollution in Natural Aquatic Systems. A Thesis Submitted for the Degree of Doctor of Philosophy

- (Environmental Pollution Science), Brunel, The University of West London, 1991.
8. M. A. Ahmad, R. Alrozi, *Chemical Engineering Journal*, **171(2)**, 510 (2011), <https://doi.org/10.1016/j.cej.2011.04.018>
 9. P. Phuengphai, Th. Singjanusong, N. Kheangkun, A. Wattanakornsiri, *Water Science and Engineering*, **14** (4), 286 (2021).
 10. S. T. Ramesh, N. Rameshbabu, R. Gandhimathi, P. V. Nidheesh, M. Srikanth Kumar, *Applied Water Science*, **2(3)**, 187 (2012), <https://doi.org/10.1007/s13201-012-0036-3>
 11. V. O. Njoku, K. Y. Foo, M. Asif, B. H. Hameed, *Chemical Engineering Journal*, **250**, 198 (2014), <https://doi.org/10.1016/j.cej.2014.03.115>
 12. H. J. Park, S. W. Jeong, J. K. Yang, B. G. Kim, S. M. Lee, *J. Environ. Sci. (China)*, **19(12)**, 1436 (2007), [https://doi.org/10.1016/S1001-0742\(07\)60234-4](https://doi.org/10.1016/S1001-0742(07)60234-4)
 13. B. Kiran, N. Rani, A. Kaushik, *International Journal of Phytoremediation*, **6514**, 1067 (2016), <https://doi.org/10.1080/15226514.2016.1183577>
 14. K. Yetilmezsoy, S. Demirel, R. J. Vanderbei, *Journal of Hazardous Materials*, **171(1-3)**, 551 (2009), <https://doi.org/10.1016/j.jhazmat.2009.06.035>
 15. L. Brahmi, F. Kaouah, S. Boumaza et al., *Applied Water Science*, **9**, 171 (2019), <https://doi.org/10.1007/s13201-019-1053-2>
 16. M. Çekim, S. Yildiz, T. Dere, *Journal of Environmental Engineering and Landscape Management*, **23(3)**, 172 (2015), <https://doi.org/10.3846/16486897.2015.1050398>.
 17. M. Farhan, A. M. Salem, N. H. Al-Dujaili, M. Awwad, *American Journal of Environmental Engineering*, **2(6)**, 188 (2012), <https://doi.org/10.5923/j.ajee.20120206.07>
 18. F. Ghorbani, H. Younesi, S. M. Ghasempouri, A. A. Zinatizadeh, M. Amini, A. Daneshi, *Chemical Engineering Journal*, **145(2)**, 267 (2008), <https://doi.org/10.1016/j.cej.2008.04.028>
 19. V. O. Njoku, K. Y. Foo, M. Asif, B. H. Hameed, *Chemical Engineering Journal*, **250**, 198 (2014), <https://doi.org/10.1016/j.cej.2014.03.115>
 20. S. Rangabhashiyam, M. S. G. Nandagopal, E. Nakkeeran, R. Keerthi, *Desalination and Water Treatment*, **3994**, 1 (2016), <https://doi.org/10.1080/19443994.2016.1163514>
 21. R. O. Cristóvão, A. P. M. Tavares, J. M. Loureiro, R. A. R. Boaventura, E. A. Macedo, *Environmental Technology*, **29(12)**, 1357 (2008), <https://doi.org/10.1080/09593330802379615>
 22. F. C. Wu, R. L. Tseng, R. S. Juang, *Chemical Engineering Journal*, **153(1-3)**, 1 (2009), <https://doi.org/10.1016/j.cej.2009.04.042>
 23. Y. Bulut, Z. Tez, *Journal of Environmental Sciences (China)*, **19(2)**, 160 (2007), [https://doi.org/10.1016/S1001-0742\(07\)60026-6](https://doi.org/10.1016/S1001-0742(07)60026-6).